HHS Public Access

Author manuscript

Nanoscale. Author manuscript; available in PMC 2017 January 10.

Published in final edited form as:

Nanoscale. 2016 May 19; 8(20): 10553–10557. doi:10.1039/c6nr01400c.

A photothermally responsive nanoprobe for bioimaging based on Edman degradation†

Yi Liu[a,b], **Zhantong Wang**[b], **Huimin Zhang**[b], **Lixin Lang**[b], **Ying Ma**[b], **Qianjun He**[b], **Nan Lu**[b], **Peng Huang**[b], **Yijing Liu**[b], **Jibin Song**[b], **Zhibo Liu**[b], **Shi Gao**[a], **Qingjie Ma**[a], **Dale O. Kiesewetter**[b], and **Xiaoyuan Chen**[b]

[a]China-Japan Union Hospital of Jilin University, Changchun, Jilin 130033, China

[b]Laboratory of Molecular Imaging and Nanomedicine (LOMIN), National Institute of Biomedical Imaging and Bioengineering (NIBIB), National Institutes of Health (NIH), Bethesda, Maryland 20892, USA

Abstract

A new type of photothermally responsive nanoprobe based on Edman degradation has been synthesized and characterized. Under irradiation by an 808 nm laser, the heat generated by the gold nanorod core breaks the thiocarbamide structure and releases the fluorescent dye Cy5.5 with increased near-infrared (NIR) fluorescence under mild acidic conditions. This RGD modified nanoprobe is capable of fluorescence imaging of $\alpha_v\beta_3$ over-expressing U87MG cells *in vitro* and *in vivo*. This Edman degradation-based nanoprobe provides a novel strategy to design activatable probes for biomedical imaging and drug/gene delivery.

There has been increased interest in developing new photoresponsive nanocarriers for controlled delivery and release of drug molecules and gene products at a specific time and location in the living system.[1] Ultraviolet (UV) light responsive photolabile protecting groups or phototriggers have been recognized as a powerful tool in biomedical applications.[2] However, the cytotoxic effect[3] and low tissue penetration depth[4] of the UV light would limit their application *in vivo*. Near-infrared (NIR) irradiation could overcome issues of auto-fluorescence and improve the depth of penetration compared to UV light.[5] Particularly, the NIR strategies based on two-photon irradiated nanoprobes[6] and upconversion nanoparticles[7] that convert low energy excitation NIR light to high energy UV emission have extended *in vitro* and *in vivo* bioapplications of photoresponsive probes.[8] For these two types of NIR photocleavageable nanoprobes, however, the low optical conversion efficiency and photoluminescence quantum yield might affect their further use.[9]

Plasmonic nanoparticles with localized surface plasmon resonance (LSPR) could have their conduction electrons coherently photoexcited to induce surface plasmon oscillations. Upon surface plasmon formation, nonradiative relaxation efficiently generated localized heat to the surface.[10] There have been some reports of using plasmonic nanoparticles to break thermally

†Electronic supplementary information (ESI) available: HPLC, MS and ^{1}H NMR spectrum. See DOI: 10.1039/c6nr01400c

Correspondence to: Qingjie Ma; Dale O. Kiesewetter; Xiaoyuan Chen.

sensitive chemical structures to release biologically relevant constituents from the surface of nanoparticles.[11] For example, Bakhtiari *et al.* reported the photothermal release of molecules from gold nanoshell surfaces through an efficient thermally responsive retro-Diels–Alder reaction.[12] In this example, the breakage of the Au–S bond[13] would release the active free thiol and/or generate free radical species that may have undesired side effects, such as biotoxicity.[14] Ultimately, the ideal photothermally responsive delivery system would show precise targeting and clean photoreaction without side products.

Edman degradation is a common method of sequencing amino acids in a peptide (Scheme S1†).[15] Our group also reported the instability of glutamic acid linked peptides coupled to NOTA through different chemical linkages based on the Edman degradation.[16] This thermally responsive degradation would be activated in the acidic extracellular pH (6.5–6.8) in the tumour milieu, or endocytic organelles (pH, 5.0–6.0) in the tumour endothelial cells.[17]

In the current study, we designed a new type of photothermally responsive nanoprobe based on the Edman degradation. We developed a nanoparticle surface energy transfer (NSET) system using Cy5.5 as the energy donor and gold nanorods (AuNRs) as the energy acceptor. The two major components were linked to mimic the thiourea of a terminal amino acid residue. Irradiation (808 nm) at pH 6 generated heat in the gold nanorod core which radiated into the thiourea structure effecting the Edman degradation to release the Cy5.5-NH_2 fluorescent dye. After the Edman degradation, NSET between Cy5.5-NH_2 and the gold nanorod would be broken to recover the NIR emission of Cy5.5 (Scheme 1). This arginine–glycine–aspartate (RGD)[18] modified nanoprobe has proven to be capable of controlled release in the $\alpha_v\beta_3$ overexpressing U87MG cells by NIR fluorescent bioimaging through receptor-mediated endocytosis. This Edman degradation-based nanoprobe provides a new design strategy for tumour bioimaging.

The preparation of the photothermally responsive nanoprobe was accomplished in three main steps. Firstly, the glutamic acid was modified with Cy5.5-NH_2 on the 1-acid and c(RGDyK) on the 5-acid to provide the NH_2-Glu(Cy5.5)-c(RGDyK) in five steps (Scheme S2, Fig. S1–9†).[19] Secondly, the CTAB coated gold nanorod was modified with TEOS and isothiocyanated silica (Si-NCS, Fig. S10†) to form isothiocyanate functionalized core–shell nanoparticles (AuNR@SiO_2-NCS).[20] Finally, this silica coated nanorod AuNR@SiO_2-NCS was covalently linked with the NH_2-Glu(Cy5.5)-c(RGDyK) to yield the AuNR@SiO_2-Glu(Cy5.5)-c(RGDyK) (Scheme S3†),[21] which eliminates the potential toxicity of breakage of the Au–S bond.

We next investigated the physical properties of AuNR@SiO_2-Glu(Cy5.5)-c(RGDyK) nanoparticles. The size of AuNR@CTAB was approximately 55.0 × 18.0 nm (Fig. 1a), and the aspect ratio was about 3.1. After modification with the Si-NCS and NH_2-Glu(Cy5.5)-c(RGDyK), the thickness of the silica shell was approximately 3.8 nm in AuNR@SiO_2-NCS and AuNR@SiO_2-Glu(Cy5.5)-c(RGDyK) (Fig. 1b & c). As shown in Fig. 1d, the AuNR@CTAB showed a broad peak at 760 nm, and that of AuNR@SiO_2-NCS was slightly red-shifted to 765 nm. After coupling of NH_2-Glu(Cy5.5)-c(RGDyK), there was a new shoulder peak at 680 nm, which belongs to the dye Cy5.5, suggesting that NH_2-Glu(Cy5.5)-c(RGDyK) was successfully attached on the surface of the silica shell. The distance between

the surface of the gold nanorod and Cy5.5 was about 3.8 nm, which is within the effective range for NSET.[22] The nanoconjugate was further characterized by zeta potential and DLS. The AuNR@CTAB nanoparticles exhibit a zeta potential of +38.5 mV due to the adsorption of cationic CTAB molecules on the AuNR surface. After modification with -NCS and NH_2-Glu(Cy5.5)-c(RGDyK), the zeta potentials were −10.1 mV and +12.7 mV, respectively (Fig. 1f), and the hydrodynamic size increased from 105.1 nm to 151.6 nm (Fig. 1d). By measuring the changes in absorbance at 680 nm, the loading concentration of Glu(Cy5.5)-c(RGDyK) was about 1.10 μM (Fig. 2a), which, by calculation, indicated approximately 5500 Glu (Cy5.5)-c(RGDyK) units per AuNR@SiO_2 (Fig. S13†).[21]

The NSET efficiency was measured by the fluorescence emission and lifetime spectroscopy. Compared with the NIR emission intensity of NH_2-Glu(Cy5.5)-c(RGDyK) at a concentration of 1.10 μM, the NIR emission intensity at 700 nm was significantly quenched for the AuNR@SiO_2-Glu(Cy5.5)-c(RGDyK) (Fig. S14†). The NSET efficiency was ~85.7%, as deduced from the emission spectra of AuNR@SiO_2-Glu(Cy5.5)-c(RGDyK). At the same time, the fluorescence lifetime of AuNR@SiO_2-Glu(Cy5.5)-c(RGDyK) was reduced from 1.2 ns to 0.7 ns (Fig. 2b), further confirming the effective quenching of the dye emission of Cy5.5 by the nanorod through the NSET process.[23] In contrast, simple physical mixing of AuNR@SiO_2-NCS and Glu(Cy5.5)-c(RGDyK) did not result in an obvious decrease in the NIR emission intensity (Fig. S15†). These results indicate that the quenching effect in AuNR@SiO_2-Glu(Cy5.5)-c(RGDyK) was mainly ascribed to the NSET process rather than simple light absorption by the nanorod.[21]

As previously discussed, the rate of the Edman degradation depends on the temperature and pH.[15] Thus, we investigated the stability of the pure Cy5.5 and nanoprobe AuNR@SiO_2-Glu(Cy5.5)-c(RGDyK) under different temperature and pH conditions. The pure Cy5.5 dye showed high stability throughout the pH range 2–10, at 80 °C for up to 40 min, and under 808 nm laser irradiation for up to 40 min (Fig. S16†). When the AuNR@SiO_2-Glu(Cy5.5)-c(RGDyK) was heated at 80 °C at different pH values (4.0–7.0), the emission was only increased over time under acidic conditions (Fig. S17†). Simultaneously, the NIR emission increased at increasing temperatures (60–100 °C) when the pH of the solution was 6.0 (Fig. S18†). These manifest successful Edman degradation on the surface of AuNR@SiO_2-Glu(Cy5.5)-c(RGDyK) under heating and acidic conditions.

The photothermal properties of AuNR@SiO_2-Glu(Cy5.5)-c(RGDyK) nanoparticles were investigated under excitation of an 808 nm laser. The temperature of the solution ($OD_{808\ nm}$ = 0.5) increased with the increasing power density of the exposed 808 nm laser (Fig. S19a†). When the laser power was 0.3 W cm^{-2}, the temperature increased to 62.3 °C following a 2 min irradiation. In addition, the AuNR@SiO_2-Glu(Cy5.5)-c(RGDyK) showed good photothermal stability with reproducible temperature increases over 4 cycles (Fig. S19b†).

The photothermally-induced Edman degradation was evaluated by fluorescence spectroscopy, HPLC, and HPLC-MS. Following the excitation of the 808 nm laser (0.2 W cm^{-2}) for 2 min at pH 6.0, the emission intensity of the solution increased immediately. Then the exposed solution was cooled to room temperature in the dark for another 2 min, the emission intensity had no obvious changes. After irradiation for 4 additional 2 min time

periods, the emission intensity increased 5.6-fold (Fig. 3a and b). This increase in fluorescence intensity is consistent with the release of approximately 5131 dye molecules (93.3%) per nanorod (Fig. S20†). As shown in Fig. S21,† the absorption result also displayed a similar released yield (90.0%). HPLC analysis showed that a new peak at 25.0 min appeared and increased with increasing laser exposure time (Fig. 3c), and the retention time was matched with the pure dye Cy5.5-NH_2 (Fig. S22†). The mass spectrum of this component showed a molecular ion at *m/z* 681.48 consistent with Cy5.5-NH_2 (calculated *m/z* 681.45), which is the predicted Edman degradation product (Fig. 3d). Thus, the constructed AuNR@SiO_2-Glu(Cy5.5)-c(RGDyK) particle performs as predicted to be an activatable fluorescent imaging agent under irradiation of the 808 nm laser at pH 6.0.

Before the application of AuNR@SiO_2-Glu(Cy5.5)-c(RGDyK) in bioimaging, the cytotoxicity of this nanomaterial was investigated by a methyl thiazolyl tetrazolium (MTT) assay. Following incubation of 10–50 μg mL^{-1} AuNR@SiO_2-Glu(Cy5.5)-c(RGDyK) for 24 h, no significant difference in the proliferation of U87MG cells was observed (Fig. S23†). The cellular viability of U87MG cells was more than 90%, indicating low cytotoxicity of AuNR@SiO_2-Glu(Cy5.5)-c(RGDyK) nanoparticles.

To demonstrate the applicability of the nanoprobe AuNR@SiO_2-Glu(Cy5.5)-c(RGDyK) for targeted bioimaging based on Edman degradation, fluorescence imaging experiments were first carried out in two different cell lines (U87MG and MCF-7). Human glioblastoma U87MG cells (high levels of integrin $\alpha_v\beta_3$) and MCF-7 cells (low levels of integrin $\alpha_v\beta_3$) were incubated with DAPI and AuNR@SiO_2-Glu(Cy5.5)-c(RGDyK) for 1 h. As shown in Fig. 4, before the irradiation of the 808 nm laser, the U87MG cells showed a very weak NIR emissive signal in the Cy5.5 channel (Fig. 4a2). With irradiation of the 808 nm laser for an increased time, the U87MG cells displayed an obviously increased NIR signal in the Cy5.5 channel (Fig. 4b2). However, the MCF-7 cells showed no obvious changes of NIR emission in the Cy5.5 channel (Fig. 4c2 & d2).

In a concurrent experiment, the U87MG cells were treated with excess c(RGDyK), in order to block specific binding, and co-incubated with AuNR@SiO_2-Glu(Cy5.5)-c(RGDyK). After irradiation with laser, the RGD-blocked cells showed no obvious changes in the NIR emission (Fig. S24 a1 & a2†). The binding specificity suggests that AuNR@SiO_2-Glu(Cy5.5)-c(RGDyK) could be used to image the integrin $\alpha_v\beta_3$ over-expressing U87MG cells through receptor-mediated endocytosis based on Edman degradation.

As previously reported, the U87MG tumour showed the characteristic acid microenvironment.[17a] Herein, the AuNR@SiO_2-Glu(Cy5.5)-c(RGDyK) was further investigated for Edman degradation in the U87MG tumour mouse model. When the tumours reached about 60 mm^3, the mice were treated with an intratumoral injection of 50 μL of nanoprobe AuNR@SiO_2-Glu(Cy5.5)-c(RGDyK) (100 μg mL^{-1}). Fluorescence imaging was employed to monitor the Edman degradation efficacy of treatment *in vivo* using a whole body optical imaging system (Fig. 5). Before the laser irradiation, the local tumour showed weak NIR emission. Under irradiation of the 808 nm laser at a power density of 0.25 W cm^{-2}, the NIR emission increased with increasing time in the local tumour. These results

indicated that nanoparticles AuNR@SiO_2-Glu(Cy5.5)-c(RGDyK) had an excellent photothermal responsive release in the U87MG tumour based on the Edman degradation.

Conclusions

In summary, we have developed a novel photothermally responsive nanoprobe based on the Edman degradation. Under irradiation of the 808 nm laser, the gold nanorod core generated and transferred the heat to the thiourea structure to release the Cy5.5-NH_2 fluorescent dye, resulting in increased NIR emission. Importantly, this nanoprobe was capable of photothermally induced release of Cy5.5-NH_2 in the $\alpha_v\beta_3$ overexpressing U87MG cells and tumour for NIR imaging. Our Edman degradation-based nanoprobe provides a novel strategy for tumour-targeted bioimaging and drug delivery *in vitro* and *in vivo*.

Supplementary Material

Refer to Web version on PubMed Central for supplementary material.

Acknowledgments

This research was supported by the National Natural Science Foundation of China (NSFC) projects (81571708, 81501506, 81401465 & 51573096), the Research Fund of Science and Technology Department of Jilin Province (20150520154JH), the Hygiene Specific Subjects of Jilin Province (SCZSY201508) and the Intramural Research Programs of the National Institute of Biomedical Imaging and Bioengineering (NIBIB), and the National Institutes of Health (NIH).

References

1. (a) Mal NK, Fujiwara M, Tanaka Y. Nature. 2003; 421:350. [PubMed: 12540896] (b) Liong M, Angelos S, Choi E, Patel K, Stoddart JF, Zink JI. J. Mater. Chem. 2009; 19:6251.(c) Vivero-Escoto JL, Slowing II, Wu C-W, Lin VSY. J. Am. Chem. Soc. 2009; 131:3462. [PubMed: 19275256]
2. Park C, Lim J, Yun M, Kim C. Angew. Chem., Int. Ed. 2008; 47:2959.
3. Kulms D, Pöppelmann B, Yarosh D, Luger TA, Krutmann J, Schwarz T. Proc. Natl. Acad. Sci. U. S. A. 1999; 96:7974. [PubMed: 10393932]
4. Meinhardt M, Krebs R, Anders A, Heinrich U, Tronnier H. J. Biomed. Opt. 2008; 13:044030. [PubMed: 19021357]
5. Frangioni JV. Curr. Opin. Chem. Biol. 2003; 7:626. [PubMed: 14580568]
6. (a) Babin J, Pelletier M, Lepage M, Allard J-F, Morris D, Zhao Y. Angew. Chem., Int. Ed. 2009; 48:3329.(b) Lin Q, Huang Q, Li C, Bao C, Liu Z, Li F, Zhu L. J. Am. Chem. Soc. 2010; 132:10645. [PubMed: 20681684]
7. (a) Carling C-J, Nourmohammadian F, Boyer J-C, Branda NR. Angew. Chem., Int. Ed. 2010; 49:3782.(b) Yan B, Boyer J-C, Branda NR, Zhao Y. J. Am. Chem. Soc. 2011; 133:19714. [PubMed: 22082025] (c) Jayakumar MKG, Idris NM, Zhang Y. Proc. Natl. Acad. Sci. U. S. A. 2012; 109:8483. [PubMed: 22582171] (d) Dai Y, Xiao H, Liu J, Yuan Q, Ma Pa, Yang D, Li C, Cheng Z, Hou Z, Yang P, Lin J. J. Am. Chem. Soc. 2013; 135:18920. [PubMed: 24279316] (e) Li W, Wang J, Ren J, Qu X. J. Am. Chem. Soc. 2014; 136:2248. [PubMed: 24467474]
8. (a) Chen G, Qiu H, Prasad PN, Chen X. Chem. Rev. 2014; 114:5161. [PubMed: 24605868] (b) Zhou J, Liu Q, Feng W, Sun Y, Li F. Chem. Rev. 2015; 115:395. [PubMed: 25492128]
9. (a) Boyer J-C, van Veggel FCJM. Nanoscale. 2010; 2:1417. [PubMed: 20820726] (b) Xu C, Zipfel W, Shear JB, Williams RM, Webb WW. Proc. Natl. Acad. Sci. U. S. A. 1996; 93:10763. [PubMed: 8855254]
10. Mackey MA, Ali MRK, Austin LA, Near RD, El-Sayed MA. J. Phys. Chem. B. 2014; 118:1319. [PubMed: 24433049]

11. (a) Yavuz MS, Cheng Y, Chen J, Cobley CM, Zhang Q, Rycenga M, Xie J, Kim C, Song KH, Schwartz AG, Wang LV, Xia Y. Nat. Mater. 2009; 8:935. [PubMed: 19881498] (b) Song J, Yang X, Jacobson O, Lin L, Huang P, Niu G, Ma Q, Chen X. ACS Nano. 2015; 9:9199. [PubMed: 26308265] (c) Song J, Pu L, Zhou J, Duan B, Duan H. ACS Nano. 2013; 7:9947. [PubMed: 24073739] (d) Song J, Huang P, Duan H, Chen X. Acc. Chem. Res. 2015; 48:2506. [PubMed: 26134093] (e) He Q, Kiesewetter DO, Qu Y, Fu X, Fan J, Huang P, Liu Y, Zhu G, Liu Y, Qian Z, Chen X. Adv. Mater. 2015; 27:6741. [PubMed: 26401893]
12. (a) Bakhtiari ABS, Hsiao D, Jin G, Gates BD, Branda NR. Angew. Chem., Int. Ed. 2009; 48:4166. (b) Zandberg WF, Bakhtiari ABS, Erno Z, Hsiao D, Gates BD, Claydon T, Branda NR. Nanomed. Nanotechnol. Biol. Med. 2012; 8:908.(c) Asadirad AM, Erno Z, Branda NR. Chem. Commun. 2013; 49:5639.
13. Jain PK, Qian W, El-Sayed MA. J. Am. Chem. Soc. 2006; 128:2426. [PubMed: 16478198]
14. Munday R. Free Radical Biol. Med. 1989; 7:659. [PubMed: 2695409]
15. Edman P. Arch. Biochem. 1949; 22:475. [PubMed: 18134557]
16. Lang L, Ma Y, Kiesewetter DO, Chen X. Mol. Pharmacol. 2014; 11:3867.
17. (a) Wang Y, Zhou K, Huang G, Hensley C, Huang X, Ma X, Zhao T, Sumer BD, DeBerardinis RJ, Gao J. Nat. Mater. 2014; 13:204. [PubMed: 24317187] (b) Ling D, Hackett MJ, Hyeon T. Nat. Mater. 2014; 13:122. [PubMed: 24452354]
18. (a) Chen X, Tohme M, Park R, Hou Y, Bading JR, Conti PS. Mol. Imaging. 2004; 3:96. [PubMed: 15296674] (b) Xie J, Chen K, Lee H-Y, Xu C, Hsu AR, Peng S, Chen X, Sun S. J. Am. Chem. Soc. 2008; 130:7542. [PubMed: 18500805] (c) Gao J, Gu H, Xu B. Acc. Chem. Res. 2009; 42:1097. [PubMed: 19476332] (d) Kim Y-H, Jeon J, Hong SH, Rhim W-K, Lee Y-S, Youn H, Chung J-K, Lee MC, Lee DS, Kang KW, Nam J-M. Small. 2011; 7:2052. [PubMed: 21688390]
19. Yan Y, Chen K, Yang M, Sun X, Liu S, Chen X. Amino Acids. 2011; 41:439. [PubMed: 20936525]
20. (a) Liu J, Li C, Li F. J. Mater. Chem. 2011; 21:7175.(b) Huang P, Lin J, Wang S, Zhou Z, Li Z, Wang Z, Zhang C, Yue X, Niu G, Yang M, Cui D, Chen X. Biomaterials. 2013; 34:4643. [PubMed: 23523428]
21. Liu Y, Chen M, Cao T, Sun Y, Li C, Liu Q, Yang T, Yao L, Feng W, Li F. J. Am. Chem. Soc. 2013; 135:9869. [PubMed: 23763640]
22. Clegg RM. Curr. Opin. Biotechnol. 1995; 6:103. [PubMed: 7534502]
23. (a) Reineck P, Gómez D, Ng SH, Karg M, Bell T, Mulvaney P, Bach U. ACS Nano. 2013; 7:6636. [PubMed: 23713513] (b) Abadeer NS, Brennan MR, Wilson WL, Murphy CJ. ACS Nano. 2014; 8:8392. [PubMed: 25062430] (c) Liu D, Huang X, Wang Z, Jin A, Sun X, Zhu L, Wang F, Ma Y, Niu G, Walker A, Chen X. ACS Nano. 2013; 7:5568. [PubMed: 23683064]

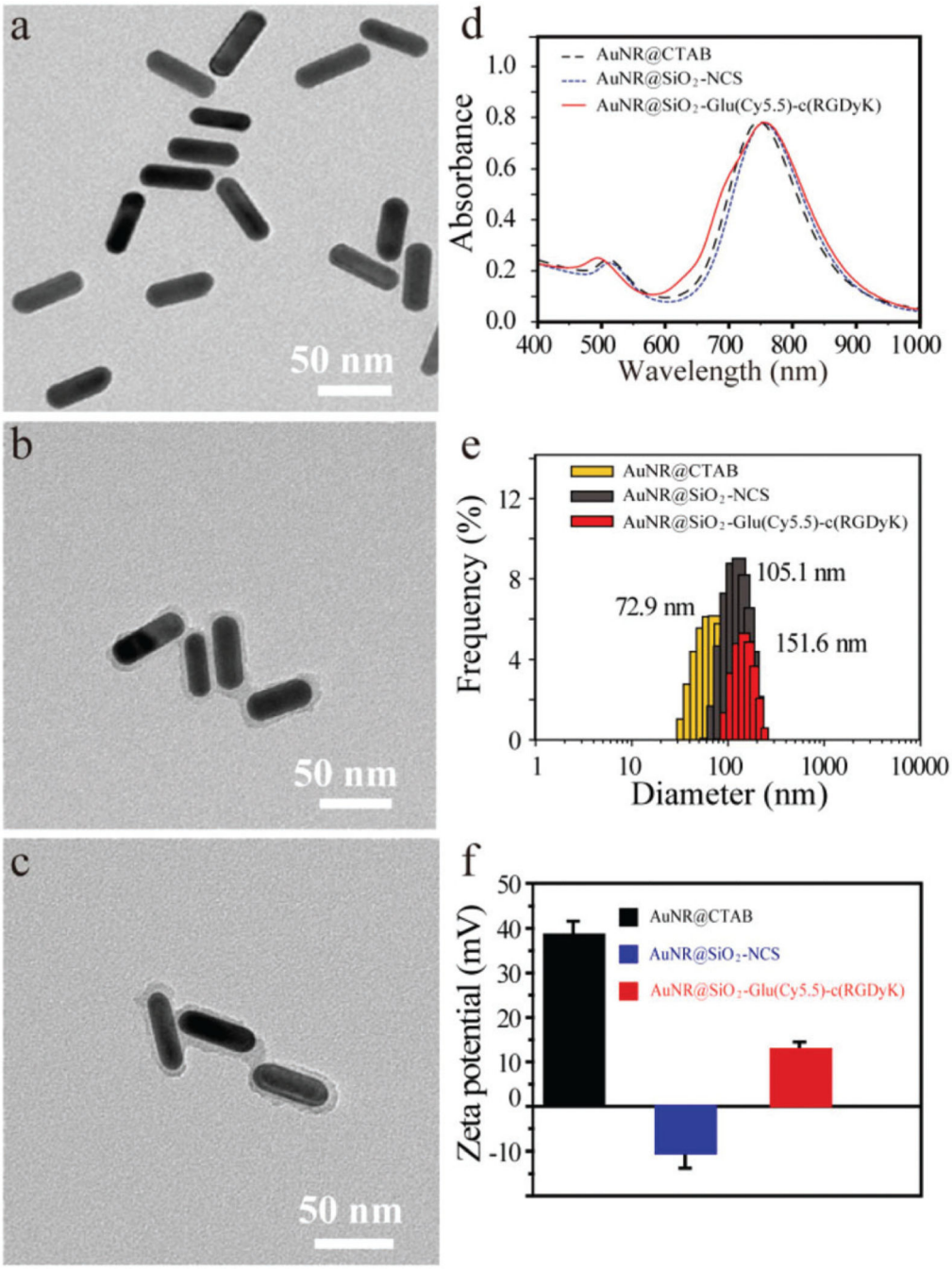

Fig. 1.

The TEM images of AuNR@CTAB (a), AuNR@SiO_2-NCS (b), AuNR@SiO_2-Glu(Cy5.5)-c(RGDyK) (c) and their corresponding absorption spectra (d), DLS (e) and zeta potentials (f).

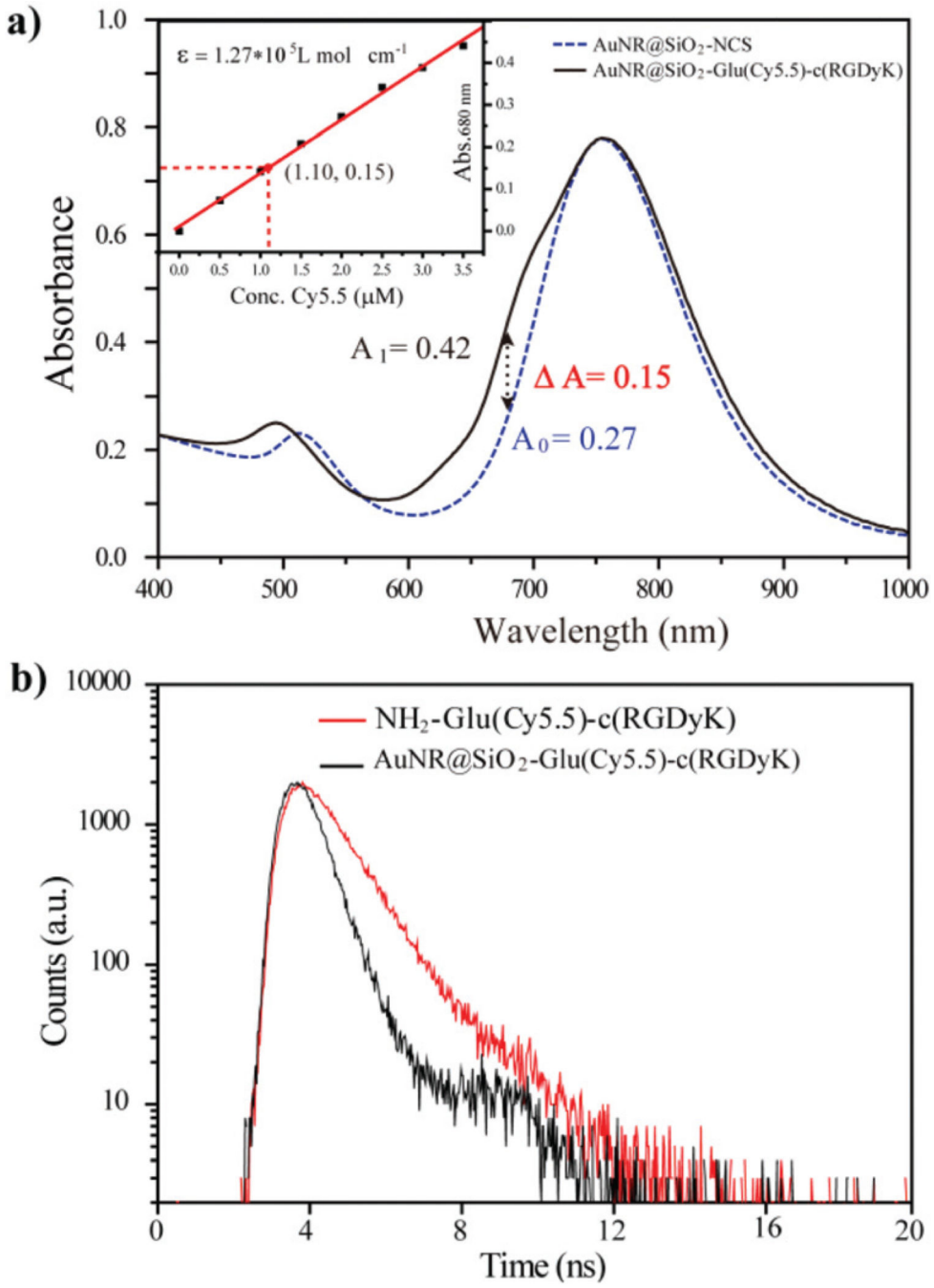

Fig. 2.

(a) The absorption spectra of AuNR@SiO_2-NCS and AuNR@SiO_2-Glu(Cy5.5)-c(RGDyK), insert: the standard curve between Abs680 nm *vs.* conc. Cy5.5; (b) the fluorescence lifetime at 700 nm of NH_2-Glu(Cy5.5)-c(RGDyK), AuNR@SiO_2-Glu(Cy5.5)-c(RGDyK).

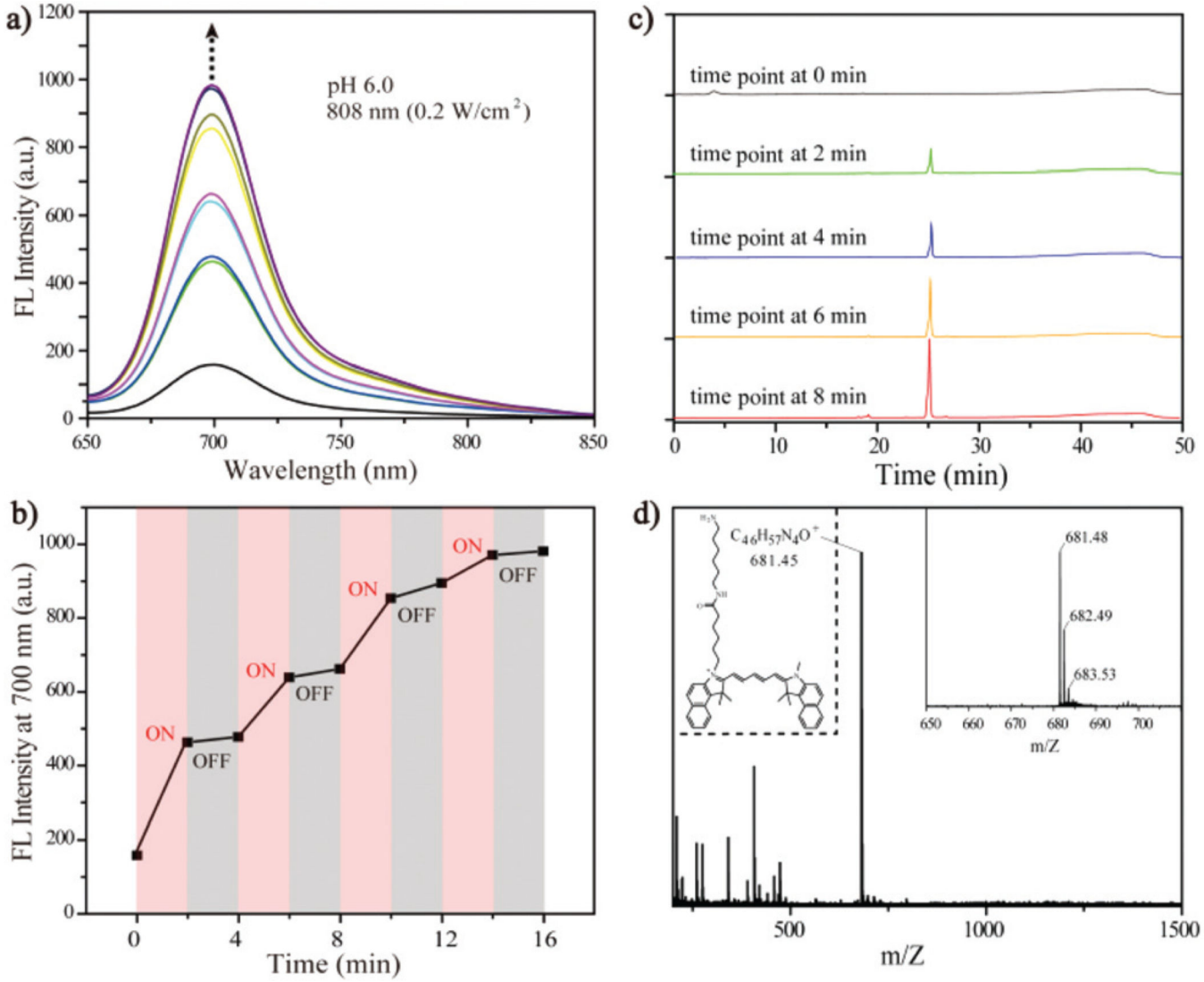

Fig. 3.

(a) The change in fluorescence of AuNR@SiO_2-Glu(Cy5.5)-c(RGDyK) following excitation with 808 nm laser (0.2 W cm^{-2}) at pH 6.0; (b) the intensity at 700 nm as a function of irradiation time; (c) their corresponding HPLC results at different time points; (d) the MS spectrum of the observed HPLC component.

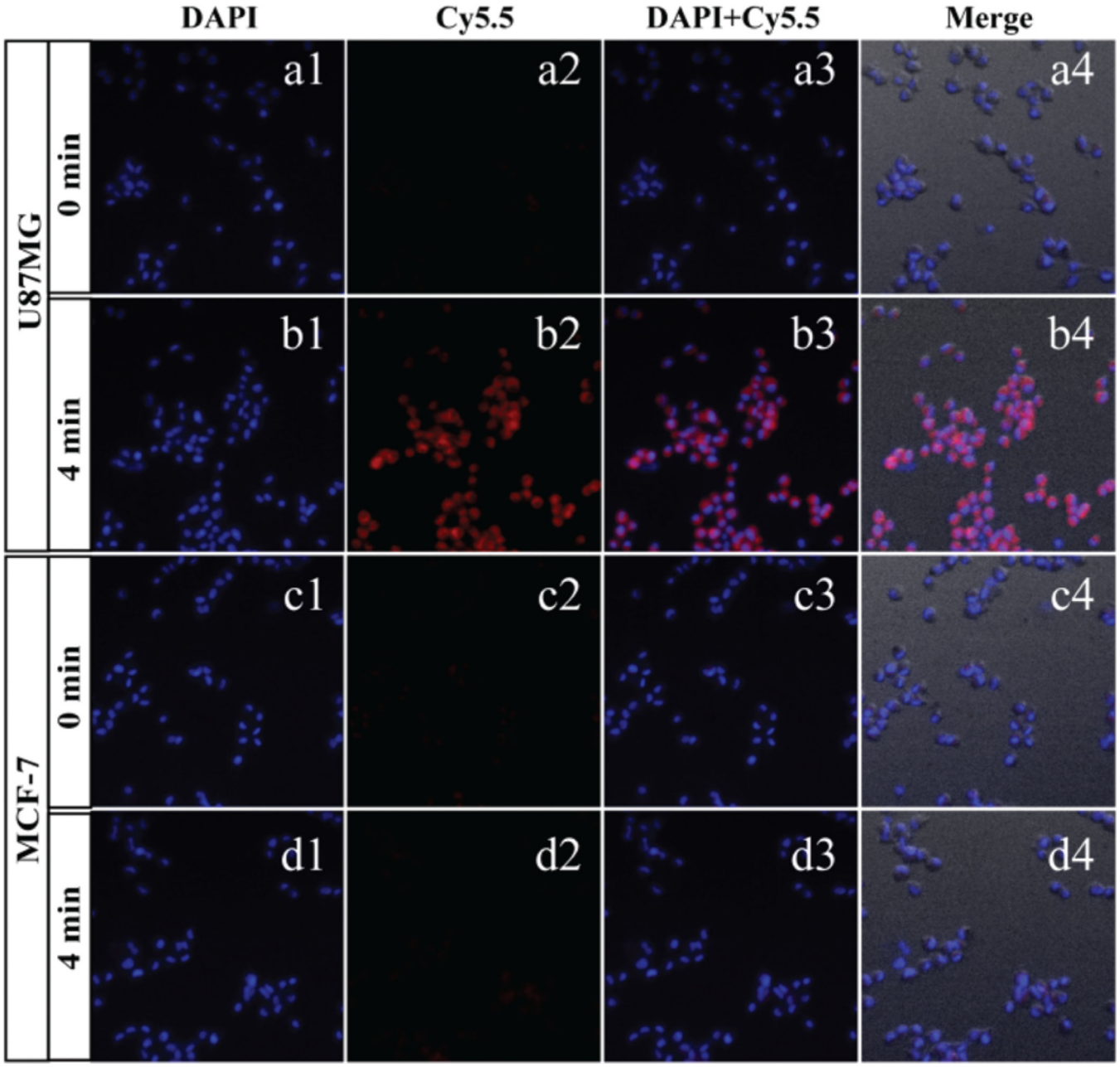

Fig. 4.

Fluorescence images of U87MG (a, b) and MCF-7 (c, d) cells treated with nanoprobe AuNR@SiO_2-Glu(Cy5.5)-c(RGDyK) (10 μg mL^{-1}) and with 808 nm laser irradiation (0.1 W cm^{-2}) for different times (0–4 min). The excitation wavelengths of DAPI and Cy5.5 were 365 and 633 nm, respectively.

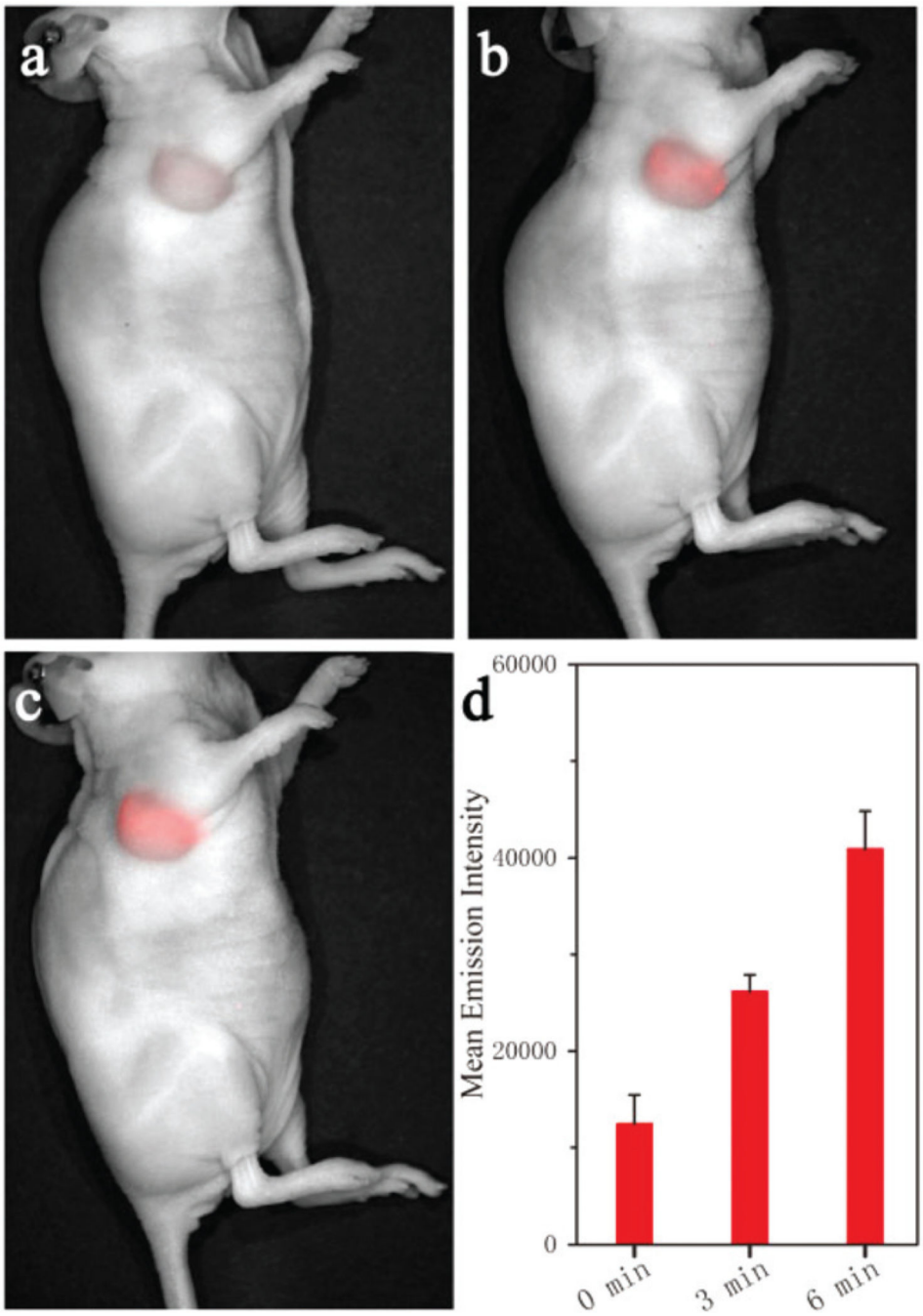

Fig. 5.

In vivo fluorescence images of U87MG tumour treated with intratumoral injection of 50 μL of AuNR@SiO_2-Glu(Cy5.5)-c(RGDyK) (100 μg mL^{-1}) under irradiation of 808 nm laser (0.25 W cm^{-2}) for 0 min (a), 3 min (b) and 6 min (c), and their corresponding changes in mean emission intensity (d). The NIR emission of Cy5.5 was collected at 650–750 nm upon irradiation at 633 nm.

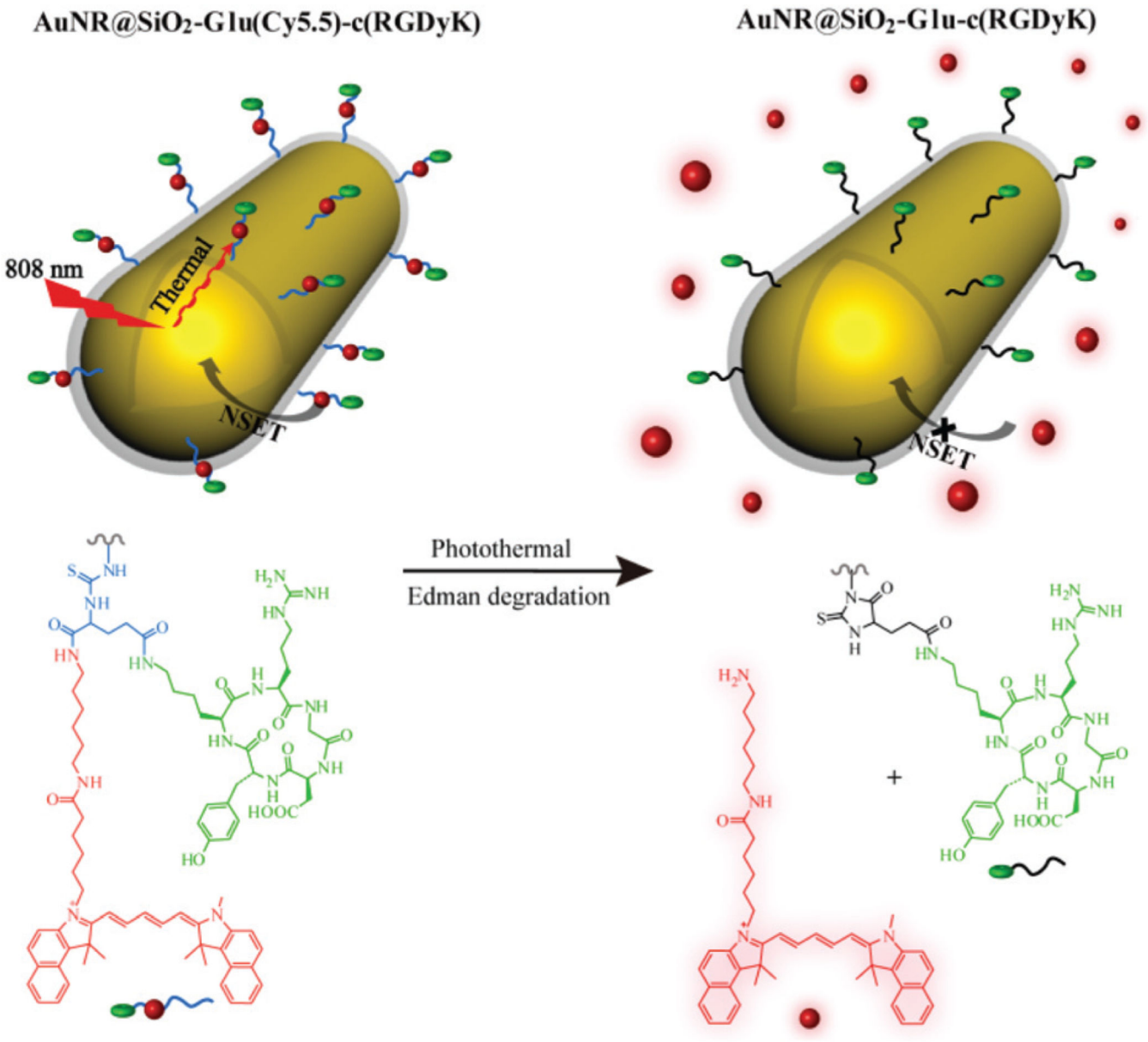

Scheme 1.

Mechanism of the photothermal decomposition of nanoprobe AuNR@SiO_2-Glu(Cy5.5)-c(RGDyK) based on the Edman degradation.